# Coordinated optimization of source-grid-load-storage for wind power grid-connected and mobile energy storage characteristics of electric vehicles

Yingliang Li[1] and Zhiwei Dong[1]

[1]Xi'an Shiyou University

July 3, 2023

**Abstract**

The rapid growth in the number of electric vehicles, driven by the 'double carbon' target, and the impact of uncontrolled charging and discharging behavior and discharged battery losses severely limit electric vehicles' low carbon characteristics. Existing research on systemic low carbon emissions and electric vehicle charging and discharging issues is usually determined by considering only carbon trading markets or charging and discharging management on the source side. In this regard, a coordinated and optimized operation model that considers the participation of electric vehicle clusters in deep peaking and the source network load and storage adjustable resources is proposed. The upper layer establishes a real-time price-based demand response model for the load side with the minimum net load fluctuation as the objective function; the middle layer establishes a comprehensive operation mechanism for the source and storage side that includes an orderly charging and discharging peaking compensation mechanism for electric vehicles and a deep peaking mechanism that takes into account clean emissions, and constructs an optimal operation model with the minimum comprehensive operating cost as the objective function; the lower layer establishes a distribution network loss minimization model for the network side that takes into account the orderly charging and discharging of electric vehicle as the objective function. The optimal tidal model with the objective function of minimizing the distribution network loss is established at the lower level. Finally, the original problem is transformed into a mixed integer linear programming problem, and the model's effectiveness is verified by setting different scenarios.

Table. 1 Electric vehicles parameter settings

| parameter | Numerical value | parameter | Numerical value |
|---|---|---|---|
| Percentage of charging electric vehicles(%) | 60 | Percentage of Discharging Electric Vehicles(%) | 30 |
| Average charge and discharge power (kW) | 1.8 | Charge and discharge frequency (day/time) | 1 |

Tab.2 Thermal power unit parameters

| Unit | Upper limit of output/MW | Lower limit of output/MW | Rate of climb/（MW·h$^{-1}$） | Carbon emissions(t/MW·h） | $a_i$ /（$·MW$^{-2}$） | $b_i$ /（$·MW） | $c_i$ /$ | Start/stop duration/h |
|---|---|---|---|---|---|---|---|---|
| G1 | 455 | 150 | 130 | 1.05 | 0.00048 | 16.19 | 1000 | 8 |
| G2 | 455 | 150 | 130 | 1.03 | 0.00031 | 17.26 | 970 | 8 |
| G3 | 130 | 20 | 60 | 0.85 | 0.002 | 16.6 | 700 | 5 |
| G4 | 130 | 20 | 60 | 0.87 | 0.0021 | 16.5 | 680 | 5 |
| G5 | 162 | 25 | 90 | 0.95 | 0.00398 | 19.7 | 450 | 6 |
| G6 | 80 | 20 | 40 | 0.74 | 0.00712 | 22.26 | 370 | 3 |
| G7 | 85 | 25 | 40 | 0.76 | 0.00079 | 27.74 | 480 | 3 |
| G8 | 55 | 10 | 40 | 0.65 | 0.00413 | 25.92 | 660 | 1 |
| G9 | 55 | 10 | 40 | 0.64 | 0.00222 | 27.27 | 665 | 1 |

Tab.3 Optimized operating solutions results for different scenarios

| Scene classification | Total cost /$ | EV discharge quantity/vehicle | Wind power consumption rate/% | Actual carbon emissions/t |
|---|---|---|---|---|
| 1 | 1,031,054.41 | 12,770 | 80.45 | 26,559.36 |
| 2 | 835,149.46 | 45,000 | 75.54 | 26,193.01 |
| 3 | 1,024,845.37 | 23,473 | 100 | 22,515.56 |
| 4 | 801,907.16 | 45,000 | 100 | 22,134.03 |

## Title of the manuscript

Coordinated optimization of source-grid-load-storage for wind power grid-connected and mobile energy storage characteristics of electric vehicles (Manuscript GTD-2023-06-0542).


## All the authors' complete names

Yingliang Li

Zhiwei Dong

## Departmental & institutional affiliations of the authors

Yingliang Li, School of Electronic Engineering, Xi'an Shiyou University, Xi'an 710065, China
Zhiwei Dong, School of Electronic Engineering, Xi'an Shiyou University, Xi'an 710065, China

## Postal & e-mail address of the corresponding author

yingliang.li@hotmail.com


## Conflict of interest statement

The authors declare that they have no known competing financial interests or personal relationships that could have appeared to influence the work reported in this paper.


## Funding information

This work was supported by the he Shaanxi Provincial Education Department Scientific Research Program Project (21JK0843) and National Natural Science Foundation of China (52174005).


## Data availability statement

The data that support the findings of this study are available from the corresponding author upon reasonable request.

## Credit contribution statement

Yingliang Li: Resources, Supervision, Project administration, Funding acquisition, Writing - Review & Editing.
Zhiwei Dong: Conceptualization, Methodology, Software, Validation, Formal analysis, Investigation, Data Curation, Writing - Original Draft.

# Coordinated optimization of source-grid-load-storage for wind power grid-connected and mobile energy storage characteristics of electric vehicles

**Yingliang Li[1a*] ,Zhiwei Dong[1b*]**

[1]School of Electronic Engineering, Xi’ an Shiyou University, Xi’ an 710065, China

[a*]yingliang.li@hotmail.com, [b*]1034203482@qq.com

Abstract—The rapid growth in the number of electric vehicles, driven by the 'double carbon' target, and the impact of uncontrolled charging and discharging behavior and discharged battery losses severely limit electric vehicles' low carbon characteristics. Existing research on systemic low carbon emissions and electric vehicle charging and discharging issues is usually determined by considering only carbon trading markets or charging and discharging management on the source side. In this regard, a coordinated and optimized operation model that considers the participation of electric vehicle clusters in deep peaking and the source network load and storage adjustable resources is proposed. The upper layer establishes a real-time price-based demand response model for the load side with the minimum net load fluctuation as the objective function; the middle layer establishes a comprehensive operation mechanism for the source and storage side that includes an orderly charging and discharging peaking compensation mechanism for electric vehicles and a deep peaking mechanism that takes into account clean emissions, and constructs an optimal operation model with the minimum comprehensive operating cost as the objective function; the lower layer establishes a distribution network loss minimization model for the network side that takes into account the orderly charging and discharging of electric vehicle as the objective function. The optimal tidal model with the objective function of minimizing the distribution network loss is established at the lower level. Finally, the original problem is transformed into a mixed integer linear programming problem, and the model's effectiveness is verified by setting different scenarios.

Keywords- Wind power consumption；Price-Based demand response；Clean emissions；Deep peaking mechanism； Electric vehicle charging and discharging

## 1. Introduction

With global climate change, the "dual carbon" strategy has gradually become the development direction of the power industry [1, 2]. Currently, China is actively promoting the carbon trading market mechanism, trying to use the market mechanism to achieve low carbon emissions in the power industry [3, 4]. On the other hand, in the context of "double carbon," electric vehicles, as a new low-carbon resource, are developing rapidly, and their disorderly charging and discharging behavior will affect the system operation, increase the net loss of the distribution network and reduce the economy and low carbon of the grid operation [5, 6]. Therefore, a suitable combination of units that considers both the carbon trading market and the orderly charging and discharging behavior of electric vehicles is of great significance to improving system economics, reducing carbon emissions, and promoting new energy consumption. In this regard, this paper proposes a comprehensive operating mechanism that simultaneously considers the carbon trading market and electric vehicles' orderly charging and discharging behavior.

With the introduction of the "double carbon" policy, the penetration rate of new energy sources has been increasing, and the peaking

capacity of the power system can hardly match the rapid development of new energy sources, leading to serious abandonment of wind and light in some areas. In the literature [7], an optimization model of peaking and frequency regulation auxiliary services considering the participation of large-scale renewable energy is proposed, which can effectively improve the utilization rate of renewable energy. In [8], a model is developed for the allocation of peaking capacity with the participation of energy storage, taking into account the uncertainty of load and wind power output, which effectively coordinates the utilization rate of new energy and system economy. In [9], a peaking auxiliary service model that takes into account the uncertainty of energy storage capacity and new energy sources is proposed to effectively reduce the pressure of system peaking. In [10], an optimal dispatch model considering the lowest market cost for deep peaking of thermal power units with the participation of multiple energy forms is proposed to optimize the operating economy of thermal power units. In [11], based on the peak and valley characteristics of the load, load characteristic constraints are added to the optimal dispatch model before the peaking day to effectively improve the load fluctuation as well as the operating economy. The above studies have conducted a lot of research on the peaking compensation strategy and peaking model for the system to participate in the peaking auxiliary services in the power market, but they have not taken into account the fact that the power system should participate in the system operation with low carbon emissions as an important indicator in the context of "double carbon".

With the increasing penetration of new energy, electric vehicles' charging, and discharging behavior management is challenging to adapt to the rapid development of new energy, leading to severe problems of wind and light abandonment problems in some regions. The literature [12] proposes a charging and discharging strategy for EVs based on charging and discharging decision functions to reduce charging demand fluctuations. In [13], a two-stage optimal scheduling model with EV charging power volatility and path planning is considered to minimize EV charging and system operation costs. In [14], an optimal scheduling model that considers EV charging and discharging power losses and charging station construction is proposed to reduce charging and discharging power losses effectively. In [15], a multi-objective optimal dispatching model is developed considering the high pollution of thermal power generation and the intermittent and fluctuating characteristics of renewable energy. The results show that the proposed strategy achieves optimal grid-connected dispatching of EVs. The literature [16] suggests a dispatching approach that uses the V2G characteristics of EVs to achieve energy supply and demand balance and achieves the optimal balance of system energy by controlling the energy flows associated with the residence, EVs, and the grid. The above studies have conducted extensive research on the participation of EVs in power system operation and their charging and discharging scheduling schemes, but they have not considered the impact of EV low-carbon output characteristics on the coordinated process of the coordinated operation method and the setting of incentives to improve the willingness of EV users to discharge, as well as the impact of orderly charging and discharging on the tidal distribution of the distribution network in the context of "double carbon".

Demand response is an effective means of load regulation to optimize the load profile. In [17], a demand response uncertainty model is developed to reduce load volatility while maintaining the economy. In [18], a price-based demand response model based on artificial neural networks is designed to improve the effectiveness of energy management strategies to address price uncertainty. In [19], a linear regression dynamic tariff scheme is constructed to enhance the comfort and economy of load users. In [20], a price-sensitive demand response model considering wind energy consumption is used to improve the flexibility and economy of unit operation. In [21], a two-tier optimized dispatch model considering a time-sharing pricing mechanism is developed to promote the balance of energy supply and demand using integrated demand response while maintaining the overall customer satisfaction within an acceptable range to exploit the potential of demand response further. The above literature

has researched the involvement of demand response in system operation, optimizing the load curve and reducing the load peak-to-valley differential. Still, due to the differences in load peak-to-valley times, the real-time tariff mechanism should guide customers to orderly electricity consumption.

From the above literature, it can be found that:

1) most references enhance the flexibility of system operation by optimizing the deep peaking mechanism, without further research on the impact of clean emissions and EV participation in deep peaking;

2) new energy consumption and EV mobile energy storage characteristics are research hotspots, but previous research on using EV mobile energy storage characteristics to promote new energy consumption is limited;

3) there is less research on using EV mobile energy storage characteristics to build a coordinated operation of source-grid-load-storage low-carbon resources.

In summary, this paper proposes a coordinated operation method considering integrated operation mechanism and demand response for EV charging and discharging management, new energy utilization, and low carbon emission of the system in the context of "double carbon." The upper layer constructs a real-time price-based demand response model for the load side to optimize the load distribution and derive the EV charging and discharging price; the middle layer takes into account the mobile energy storage characteristics of EV clusters and considers the EV orderly charging and discharging peaking compensation mechanism and the deep peaking mechanism considering clean emissions for the source and storage sides to obtain thecoordinated operation method and EV charging and discharging time scheme that meets low carbon and economy; the lower layer is based on the impact of EV charging and discharging method on the distribution network tide distribution. The lower layer is based on the impact of the EV charging and discharging scheme on the distribution of the distribution network tide. The charging and discharging space distribution scheme is obtained. Finally, we establish the unit combination model for different scenarios and prove that the model can effectively reduce the actual carbon emission, system operation cost, and network loss of the distribution network and enhance the capacity of new energy consumption.

The main contributions of this study can be summarized as

1. Build a coordinated operation model of source-grid, load and storage that takes into account the mobile energy storage characteristics of electric vehicles, to improve the economy and low carbon of system operation, to reduce the network loss of distribution network operation, and to strengthen the connection between source-grid, load and storage resources;

2. Propose a deep peaking mechanism considering clean emissions, improve the operational flexibility of thermal power units, increase the consumption rate of new energy and reduce unit operating costs;

3. Propose an orderly charging and discharging peaking compensation mechanism that takes into account the cost of electric vehicle discharging losses to enhance the willingness of electric vehicle users to participate in discharging, reduce the cost of charging and discharging for vehicle owners, and assist thermal power units in peaking.

## 2. Operational framework for integrated service mechanisms and demand response with EV

### *2.1. Analysis of real-time price-based demand response models*

In the context of "double carbon", the economic and low carbon constraints are not to be ignored in the unit mix. In this paper, we start from the source network, load storage, and resources and use the price-based demand response and integrated operation mechanism to construct the unit mix framework.

$$e_{i,j} = \frac{\Delta Q_i / Q_i^0}{\Delta \rho_j / \rho_j^0} \tag{1}$$

Where: $e_{i,j}$ - moment $i$ load to moment $j$ tariff elasticity coefficient, $\Delta Q$ - the amount of load change at the moment $i$ after the demand response, $\Delta \rho_j$ - the initial amount of $j$

moment load, for the amount of tariff change at the moment after the demand response, $\rho_j^0$ - the initial amount of tariff at the $j$ moment.

The relationship between the amount of change in electricity and the amount of change in tariff after the implementation of peak and valley tariffs is

$$\begin{bmatrix} \Delta Q_1 / Q_1^0 \\ \Delta Q_2 / Q_2^0 \\ \vdots \\ \Delta Q_i / Q_i 0 \end{bmatrix} = E_{ij} \cdot \begin{bmatrix} \Delta \rho_1 / \rho_1^0 \\ \Delta \rho_2 / \rho_2^0 \\ \vdots \\ \Delta \rho_i / \rho_i^0 \end{bmatrix} \tag{2}$$

Where: $E_{ij}$ - Price elasticity of demand matrix.

Then the price-based demand response model in this paper is

$$\begin{bmatrix} Q_1^{'} \\ Q_2^{'} \\ \vdots \\ Q_i^{'} \end{bmatrix} = \begin{bmatrix} Q_1^0 & 0 & \cdots & 0 \\ 0 & Q_2^0 & \cdots & 0 \\ \vdots & \vdots & & \vdots \\ 0 & 0 & \cdots & Q_i^0 \end{bmatrix} \cdot E_{ij} \cdot \begin{bmatrix} \Delta \rho_1 / \rho_1^0 \\ \Delta \rho_2 / \rho_2^0 \\ \vdots \\ \Delta \rho_i / \rho_i^0 \end{bmatrix} + \begin{bmatrix} Q_1^0 \\ Q_2^0 \\ \vdots \\ Q_i^0 \end{bmatrix} \tag{3}$$

Where: $Q_i^{'}$ - Electricity after demand response.

### *2.2. Analysis of deep peaking mechanism considering clean emissions*

At present, the peaking market mainly contains deep peaking, start-stop peaking and shutdown peaking, etc. This paper mainly considers deep peaking auxiliary services. The power market can use deep peaking auxiliary services to compensate the peaking units for participating in the deep peaking process, and the power market will compensate according to the depth of peaking units according to the ladder type offer.

The peaking process of thermal power units is divided into regular peaking and deep peaking, and the cost of regular peaking is the cost of coal consumption without the compensation benefit of peaking.

$$C_{1,i,t} = a_i P_{i,t}^2 + b_i P_{i,t} + c_i \tag{4}$$

Where: $C_{1,i,t}$ - conventional peaking cost of unit $i$ at moment $t$, $P_{i,t}$ - unit $i$ output at moment $t$, $a_i$、$b_i$、$c_i$ - coal consumption coefficient of thermal power units.

In the process of deep peaking without oil injection it is necessary to consider the unit life loss cost cost of thermal power units, which is given by

$$N_{i,t} = 0.005778 P_{i,t}^3 - 2.682 P_{i,t}^2 + 484.8 P_{i,t} - 8411 \tag{5}$$

Where: $N_{i,t}$ -the rotor cracking cycle of unit i at time t , When the deep peaking unit output is less than the minimum value of conventional peaking output, the life loss of thermal units is calculated.

$$C_{2,i,t} = L \frac{C_{\text{th},i}}{2N_{i,t}} \tag{6}$$

Where: $C_{2,i,t}$ - the loss cost of the deep peaking phase of unit i at time t, $L$ - the operating loss factor of the unit, $C_{\text{th},i}$ - the purchase cost of the unit.

When the unit enters the deep peak fueling stage, it needs to be fueled, thus bringing additional fueling cost, the equation is

$$C_{3,i,t} = Q_{\text{o}} C_{\text{o}} \tag{7}$$

Where: $C_{3,i,t}$ - the cost of oil input at the deep peaking stage of unit i at time t, $Q_{\text{o}}$ - the oil consumption of oil input to fuel the deep peaking of thermal power units, $C_{\text{o}}$ - the fuel oil price.

The operating costs of the peaking units in the system at different stages of operation can be described by a segmented linear function, whose equation is

$$C_{i,t} = \begin{cases} C_{1,i,t} & ,P_{\text{G1}} \le P_{i,t} \le P_{\text{G0}} \\ C_{1,i,t} + C_{2,i,t} & ,P_{\text{G2}} \le P_{i,t} \le P_{\text{G1}} \\ C_{1,i,t} + C_{2,i,t} + C_{3,i,t} & ,P_{\text{G3}} \le P_{i,t} \le P_{\text{G2}} \end{cases} \tag{8}$$

Where: $C_{i,t}$ - the cost of peaking stage of unit i at time t, $P_{\text{G0}}$, $P_{\text{G1}}$, $P_{\text{G2}}$, $P_{\text{G3}}$ - the maximum value of regular peaking output, the minimum value of regular peaking output, the minimum value of non-oil-operated output, the minimum value of oil-operated output.

The peaking benefits of system participation in deep peaking are

$$C_{\text{d,p},i} = \begin{cases} \sum_{i=1}^{M} \sum_{t}^{T} (k_1 (P_{G1} - P_{i,t})), P_{\text{G2}} \le P_{i,t} \le P_{\text{G1}} \\ \sum_{i=1}^{M} \sum_{t}^{T} (k_{\text{t}} + k_2 (P_{G2} - P_{i,t})), P_{\text{G3}} \le P_{i,t} \le P_{\text{G2}} \end{cases} \tag{9}$$

Where: $C_{\text{d,p},i}$ - deep peaking compensation revenue, $k_1$, $k_2$ - deep peaking without oil stage unit power generation compensation price, deep peaking with oil stage unit power generation compensation price, $k_{\text{t}}$ - deep peaking without oil stage total compensation revenue.

In order to adapt to the development trend of clean energy, the Kyoto Protocol of the United Nations Framework Convention on Climate Change defines a clean energy strategy, and it is necessary to incorporate clean emissions into the deep peaking model of the system, while considering the economy and low carbon of the system operation.

In this paper, the baseline method is used to allocate the initial carbon emission allowances for the system, which is calculated by the following formula:

$$E_{\mathrm{D},t} = \sum_{t=1}^{T} \lambda(\sum_{i=1}^{M} P_{i,t} + P_{\mathrm{w},t} + P_{\mathrm{ED},t}) \quad (10)$$

Where: $E_{\mathrm{D},t}$ - the total carbon emission allowance of the system, $P_{i,t}$ - the output of thermal power units at moment t, $P_{\mathrm{w},t}$ - the output of wind power units at moment t, and $P_{\mathrm{ED},t}$ - the output of EV at moment t.

Considering the Clean Emissions Mechanism, the carbon cost of the system is

$$C_{\mathrm{c},t}=\begin{cases} K_{\mathrm{CDM}}E_{\mathrm{CDM},t}^{\max}+K_{\mathrm{p}}(E_{\mathrm{c},t}-E_{\mathrm{D},t}-E_{\mathrm{CDM},t}^{\max}) & 0<E_{\mathrm{CDM},t}^{\max}<E_{\mathrm{D},t}-E_{\mathrm{c},t} \\ K_{\mathrm{CDM}}(E_{\mathrm{c},t}-E_{\mathrm{D},t}) & 0<E_{\mathrm{D},t}-E_{\mathrm{c},t}<E_{\mathrm{CDM},t}^{\max} \\ -K_{\mathrm{CDM}}(E_{\mathrm{D},t}-E_{\mathrm{c},t}) & 0<E_{\mathrm{c},t}-E_{\mathrm{D},t}<E_{\mathrm{CDM},t}^{\max} \\ -K_{\mathrm{CDM}}E_{\mathrm{CDM},t}^{\max} & 0<E_{\mathrm{CDM},t}^{\max}<E_{\mathrm{c},t}-E_{\mathrm{D},t} \end{cases} \quad (11)$$

Where: $K_{\mathrm{CDM}}$ - the price per unit of carbon emissions traded under the Clean Emission Mechanism; $K_{\mathrm{p}}$ - the penalty per unit of excess emissions under the Clean Emission Mechanism; $E_{\mathrm{CDM},t}^{\max}$ - the upper limit of emission credits traded by the system through the Clean Emission Mechanism in the tth time period, allocated according to the load share in the operation cycle; $E_{\mathrm{c},t}$ - the actual carbon emissions in the tth time period.

In summary, the cost of a deep peaking mechanism considering clean emissions is

$$C_{\mathrm{P}} = C_{i,t} + C_{\mathrm{d,p},i} + C_{\mathrm{c},t} \quad (12)$$

Where: $C_{\mathrm{P}}$ - the cost of deep peaking considering clean emissions at time period t.

### *2.3. Analysis of orderly charging and discharging peaking compensation mechanism for electric vehicles*

As an important low-carbon resource, EV charging and discharging behavior will affect the system. EV orderly charging and discharging peaking compensation mechanism, using different charging and discharging prices to guide EV charging and discharging management, and because discharging behavior will lead to battery loss, set up a ladder compensation to improve users' willingness to discharge, participate in deep peaking through discharging behavior to gain revenue, and arbitrage in the power market to reduce system operating costs, reduce carbon emissions and optimize distribution of tidal currents in the distribution network, Reduce carbon emissions and optimize the distribution of tidal currents in the distribution network. Considering the peaking compensation mechanism of EVs, it strengthens the connection between low-carbon resources and thermal power units and promotes the rationalization of energy structure, and the parameters of EVs are set as in Table 1.

The total charging and discharging costs of electric vehicles are

$$C_{\mathrm{E}} = e_{c,t}P_{\mathrm{EC},t} + C_{\mathrm{BAT}}P_{\mathrm{ED},t} \quad (13)$$

$$\begin{cases} P_{\mathrm{EC},t} = N_{c,t}P_c\Delta t \\ P_{\mathrm{ED},t} = N_{d,t}P_d\Delta t \end{cases} \quad (14)$$

Where: $C_{\mathrm{E}}$ - the total charging and discharging cost of the electric vehicle during time period t; $P_{\mathrm{EC},t}$ - electric vehicle charging load during time period t; $C_{\mathrm{BAT}}$ - EV discharge battery depletion cost factor; $e_{c,t}$ 、 $e_{d,t}$ - the charging and discharging price of the electric vehicle during time period t; $N_{c,t}$ 、 $N_{d,t}$ - the total number of electric vehicles charged and discharged at time slot t; $P_c$ 、 $P_d$ -the average charging power and discharging power of electric vehicles; $\Delta t$ - the duration of time slot t.

As EVs impact battery life when discharged, some EV users are reluctant to discharge, so an orderly discharge incentive compensation mechanism can attract users to discharge. The cost of charging and discharging EVs is

$$C_{\mathrm{J}}=\begin{cases} e_{d,t}P_{\mathrm{ED},t} & ,0\le P_{\mathrm{ED},t}\le 0.4P_{\mathrm{ED,max}} \\ e_{d,t}P_{\mathrm{ED},t}+kP_{\mathrm{ED},t} & ,0.4P_{\mathrm{ED,max}}\le P_{\mathrm{ED},t}\le 0.6P_{\mathrm{ED,max}} \\ e_{d,t}P_{\mathrm{ED},t}+k(1+\mathrm{J})\ P_{\mathrm{ED},t} & ,0.6P_{\mathrm{ED,max}}\le P_{\mathrm{ED},t}\le 0.8P_{\mathrm{ED,max}} \\ e_{d,t}P_{\mathrm{ED},t}+k(1+2\mathrm{J})\ P_{\mathrm{ED},t} & ,0.8P_{\mathrm{ED,max}}\le P_{\mathrm{ED},t}\le P_{\mathrm{ED,max}} \end{cases} \quad (15)$$

Where: $C_{\mathrm{J}}$ - Electric vehicle discharge gain during time period t; $e_{d,t}$ - the discharge price

of the electric vehicle during time period t; $P_{\mathrm{ED,max}}$ - Maximum discharge power of electric vehicles; k - electric vehicle discharge compensation price; J - Discharge compensation growth rate for electric vehicles.

$$C_{\mathrm{EB}} = C_{\mathrm{E}} + C_{\mathrm{J}} \tag{16}$$

Where: $C_{\mathrm{EB}}$ - Total cost of charging and discharging electric vehicles in time period t.

Table. 1 Electric vehicles parameter settings

| parameter | Numerical value | parameter | Numerical value |
|---|---|---|---|
| Percentage of charging electric vehicles(%) | 60 | Percentage of Discharging Electric Vehicles(%) | 30 |
| Average charge and discharge power (kW) | 1.8 | Charge and discharge frequency (day/time) | 1 |

## 3. Coordinated operation model of integrated operation mechanism considering low-carbon characteristics of EV

With the implementation of the national "dual carbon" policy, the power system needs to be regulated from multiple resources to enhance the low-carbon nature of the power system. To this end, this paper constructs a three-stage optimal operation model that considers demand response, deep peaking with clean emissions and orderly charging and discharging peaking compensation mechanism to meet the needs of the power system, taking into account the source network load and storage resources.The optimized operation model is shown in Figure 1.

### *3.1. Model objective function*

3.1.1 Upper-level objective function

The upper-level model starts from the load side, optimizes the net load curve, and adopts a real-time tariff strategy to guide customers' electricity consumption behavior, with minimum net load fluctuation as the objective function.

$$f = \min \sum_{t=1}^{T} \left(P_{\mathrm{eq},t} - P_{\mathrm{eqv}}\right)^2 \tag{17}$$

$$P_{\mathrm{eq},t} = P_{\mathrm{L},t} - P_{\mathrm{w},t} \tag{18}$$

$$P_{\mathrm{eqv}} = \frac{1}{T}\sum_{t=1}^{T} P_{\mathrm{eq},t} \tag{19}$$

Where: $f$ - net load fluctuation; $P_{\mathrm{eq},t}$ - momentary $t$ net load; $P_{\mathrm{eqv}}$ - net load average, $P_{\mathrm{L},t}$ - momentary $t$ electrical load.

3.1.2 Mid-level objective function

The optimized load $P_{\mathrm{D}t}$ and real-time electricity prices $\rho_t$ obtained from the upper model is substituted into the middle model, which optimizes the source and storage side, and constructs the objective function with the lowest comprehensive cost by considering the unit generation cost, electric vehicle charging and discharging cost, wind power operation and maintenance cost, wind abandonment cost, and the cost of carbon trading market.

$$C = \min(C_1 + C_2 + C_3 + C_4) \tag{20}$$

Where: $C$ - total cost of unit combination model, $C_1$ - generation cost of thermal units, $C_2$ - cost of participating in the integrated service mechanism, $C_3$ - cost of wind power operation and maintenance, $C_4$ - cost of wind abandonment penalty.

(1) Generation cost of thermal power units

$$C_1 = \sum_{i=1}^{M}\sum_{t=1}^{T}\left(C_i^{\mathrm{f}}(P_{i,t}) + C_i^{\mathrm{U}}\right) \tag{21}$$

$$C_i^{\mathrm{f}}(P_{i,t}) = a_i P_{i,t}^2 + b_i P_{i,t} + c_i \tag{22}$$

$$C_i^{\mathrm{U}} = u_{i,t}(1-u_{i,t-1})G_i \tag{23}$$

Where:, $C_i^{\mathrm{f}}(P_{i,t})$ 、 $C_i^{\mathrm{U}}$ - the unit coal consumption cost, start and stop cost, $u_{i,t}$ - the start and stop state of the unit at the moment of $t$ , as 0-1 variable, 0 is the stop state, 1 is the start state, $G_i$ - the single unit start and stop cost.

(2) Cost of participation in integrated mechanisms

$$C_2 = C_{\mathrm{EB}} + C_{\mathrm{P}} \tag{24}$$

(3) Wind power operation and maintenance costs

$$C_3 = \sum_{t=1}^{T} S_{\mathrm{w}} P_{\mathrm{w},t} \tag{25}$$

(4) Wind Abandonment Costs

$$C_4 = \sum_{t=1}^{T} k_{\mathrm{w}}\left(P_{\mathrm{w}} - P_{\mathrm{w},t}\right) \tag{26}$$

Where: $k_{\mathrm{w}}$ - the cost of wind abandonment penalty per unit of electricity generated by wind power, $P_{\mathrm{w}}$ - the projected power generated by wind power.

Where: $S_{\mathrm{w}}$ - the operation and maintenance costs of wind power output unit power

generation, $P_{w,t}$ - the actual power generated by wind power at the moment of $t$.

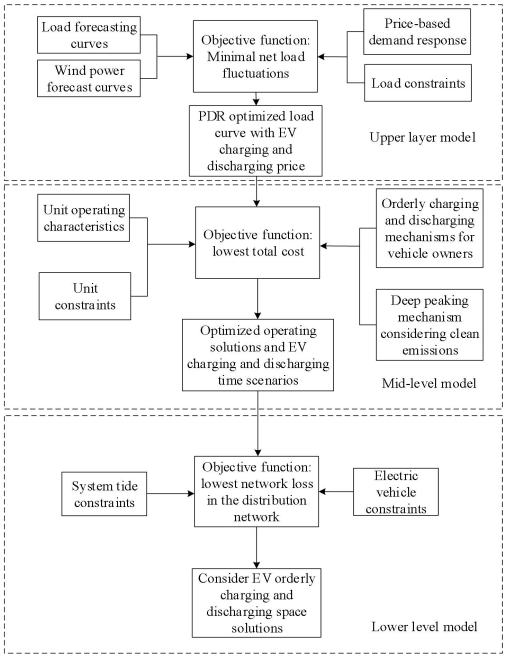


Fig.1 A three-stage optimal operation model of source-grid-load-storage considering the mobile energy storage characteristics of electric vehicles

3.1.3 Lower-level objective function

The lower layer model starts from the network side, optimizes the distribution of distribution network tide based on the optimal tide, and determines the spatial distribution scheme of EV charging and discharging nodes in the distribution network by the charging and discharging time distribution scheme obtained from the middle layer model, with the minimum network loss of the distribution network as the objective function.

$$g = \min \sum_{t=1}^{T} \sum_{ij \in E} I_{ij,t}^2 r_{ij} \tag{27}$$

Where: $g$ - the active network loss of distribution network; $E$ - the collection of distribution network branches; $I_{ij,t}$ - the branch $ij$ current at the moment of $t$; $r_{ij}$ - the branch $ij$ resistance.

### *3.2. Model Constraints*

3.2.1 Upper Level Constraints

$$\sum_{t=1}^{T} P_{L,t} = \sum_{t=1}^{T} P_{D,t} \tag{28}$$

$$-\alpha \cdot P_{L,t} \le \Delta P_{D,t} \le \alpha \cdot P_{L,t} \tag{29}$$

$$-\beta \cdot \rho_t^0 \le \Delta \rho_t \le \beta \cdot \rho_t^0 \tag{30}$$

$$\sum_{t=1}^{T} P_{D,t}(\rho_t^0 + \Delta \rho_t) \le \sum_{t=1}^{T} P_{L,t} \rho_t^0 \tag{31}$$

Eqs. (28), (29), (30), (31) represent the response power balance constraint, response power constraint, tariff change constraint, and customer cost constraint, where, $P_{D,t}$ - the demand response load at $t$ moments; $\alpha$ - the upper limit of load response at each moment; $\Delta P_{D,t}$ - the load change at $t$ moments after the response; $\beta$ - the upper limit of tariff change at each moment.

3.2.2 Mid-level constraints

$$P_{D,t} + P_{EC,t} = P_{w,t} + P_{ED,t} + \sum_{t=1}^{M} P_{i,t} \tag{32}$$

$$\begin{cases} 0 \le P_{i,t} \le P_{G,\max} \\ 0 \le P_{w,t} \le P_{w,\max} \end{cases} \tag{33}$$

$$-R_d \le P_{i,t} - P_{i,t-1} \le R_u \tag{34}$$

$$\begin{cases} \sum_{k=t}^{t+T_S-1} (1-u_{i,k}) \ge T_S(u_{i,t-1} - u_{i,t}) \\ \sum_{k=t}^{t+T_O-1} u_{i,k} \ge T_O(u_{i,t} - u_{i,t-1}) \end{cases} \tag{35}$$

$$C_{i,t}^{U} \ge G_i(U_{i,t} - U_{i,t-1}) \ge 0 \tag{36}$$

$$\sum_{i=1}^{M} (u_{i,t} P_{G,\max}) + P_{w,t} + P_{EB,t} \ge P_{L,t} + P_{EC,t} + R_t \tag{37}$$

$$\begin{cases} 0 \le N_{c,t} \le N_{c,t}^{\max} \\ 0 \le N_{d,t} \le N_{d,t}^{\max} \end{cases} \tag{38}$$

$$\begin{cases} \sum_{t=1}^{T} N_{c,t} \Delta t = N_c^{\max} \Delta t_c \\ \sum_{t=1}^{T} N_{d,t} \Delta t \le N_d^{\max} \Delta t_d \end{cases} \tag{39}$$

Eqs. (32), (33), (34), (35), (36), (37), (38), (39) represent the power balance constraint, unit output constraint, unit climbing constraint, unit start/stop time constraint, unit start/stop cost constraint, rotation standby constraint, EV chargeable quantity constraint, EV charge/discharge demand constraint, respectively.where, $M$ - the total number of units; $P_{G,\max}$ - the maximum rated power generation of thermal units; $P_{w,\max}$ - the maximum rated power generation of wind power;, $R_d$ 、 $R_u$ - the down and up climb rate limits of thermal units;, $T_S$ 、 $T_O$ - the minimum

unit shutdown time and start-up time; $G_i$ - the single start-up cost of $i$ units at the moment of $t$; $R_t$ - the rotating reserve factor of the system at the moment of $t$;, $N_{c,t}^{\max}$、$N_{d,t}^{\max}$ - the maximum number of EVs that can be charged and discharged at the moment of $t$;, $N_c^{\max}$、$N_d^{\max}$ - the total number of all EVs that can be charged and discharged; $\Delta t_c$、$\Delta t_d$ - the average charging and discharging time.

3.2.3 Lower Level Constraints

$$P_{Gi,t} + P_d N_{di,t} - P_{Di,t} - P_c N_{ci,t} - P_{Ti,t} = 0 \quad (40)$$

$$Q_{Gi,t} - Q_{Di,t} - Q_{Ti,t} = 0 \quad (41)$$

$$V_{i,\min} \le V_{i,t} \le V_{i,\max} \quad (42)$$

$$I_{ij,\min} \le I_{ij,t} \le I_{ij,\max} \quad (43)$$

$$P_{ij,\min} \le P_{ij,t} \le P_{ij,\max} \quad (44)$$

$$0 \le N_{ci,t} + N_{di,t} \le N_{i,\max} \quad (45)$$

$$\begin{cases} \sum_{i \in A} N_{ci,t} = N_{c,t} \\ \sum_{i \in A} N_{di,t} = N_{d,t} \end{cases} \quad (46)$$

Eqs. (40) and (41) denote the node power balance constraint; Eq. (42) denotes the node voltage magnitude constraint; Eq. (43) denotes the branch current constraint; Eq. (44) denotes the branch power transmission constraint; Eq. (45) denotes the node charging and discharging capacity constraint; Eq. (46) denotes the electric vehicle charging and discharging quantity constraint.where, $P_{Gi,t}$、$N_{di,t}$、$P_{Di,t}$、$N_{ci,t}$、$P_{Ti,t}$ - the active power emitted by the active source of the node $i$ at the moment $t$, the number of discharged cars of the node $i$ at the moment $t$, the active load of the node $i$ at the moment $t$, the number of charged cars of the node $i$ at the moment $t$, the transmitted active power of the node $i$ at the moment $t$, $Q_{Gi,t}$、$Q_{Di,t}$ $Q_{Ti,t}$ - the reactive power emitted by the reactive source of the node $i$ at the moment $t$ moment reactive power from the reactive power source at node $i$, $t$ moment reactive load at node $i$, $t$ moment transmitted reactive power at node $i$, $V_{i,\min}$、$V_{i,\max}$ - minimum and maximum values of voltage at node $i$, $I_{ij,\min}$、$I_{ij,\max}$ - minimum and maximum values of current at branch $ij$; $P_{ij,\min}$、$P_{ij,\max}$ --the minimum, maximum value of the transmitted power of the branch $ij$; $N_{i,\max}$ --the maximum number of charging and discharging vehicles of the node $i$; $A$ --the collection of distribution network nodes.

## 4. Example analysis

### *4.1. Basic data and parameters*

In this paper, a modified 10-unit transmission system with IEEE 33-node distribution network is used for arithmetic analysis. The transmission system consists of 9 thermal units with 1 large 120 MW wind farm, the wind farm replaces thermal unit 10, unit 1 is a deep peaking unit, and the unit parameters are shown in Table 2.

In this paper, the carbon trading base price is set at 25 $/t, and the baseline carbon emission factor for this system is 0.75; the wind power operation and maintenance cost is selected as 30 $/MW • h, the abandoned wind penalty cost is 100 $/MW •h; thermal power units participate in deep peaking auxiliary service price of $k_1$ is 40 $/MW, $k_2$ is 80 $/MW, the operating loss factor of the unit without oil deep peaking stage is 1.2, and the operating loss factor of the oil deep peaking stage is 1.5; there are 150,000 electric vehicles in this transmission system, the battery loss cost is 150 $/MW • h, the discharge compensation base price is 100 $/MW, J = 50% load and wind power forecast data is shown in Figure 2.

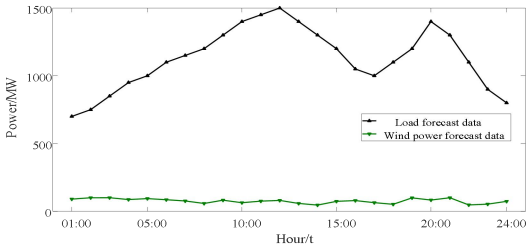


Fig.2 Load and wind power forecasting

Tab.2 Thermal power unit parameters

| Unit | Upper limit of output/MW | Lower limit of output/MW | Rate of climb/（MW·h$^{-1}$） | Carbon emissions(t/MW·h） | $a_i$ /（$·MW$^{-2}$） | $b_i$ /（$·MW） | $c_i$ /$ | Start/stop duration/h |
|---|---|---|---|---|---|---|---|---|
| G1 | 455 | 150 | 130 | 1.05 | 0.00048 | 16.19 | 1000 | 8 |
| G2 | 455 | 150 | 130 | 1.03 | 0.00031 | 17.26 | 970 | 8 |
| G3 | 130 | 20 | 60 | 0.85 | 0.002 | 16.6 | 700 | 5 |
| G4 | 130 | 20 | 60 | 0.87 | 0.0021 | 16.5 | 680 | 5 |
| G5 | 162 | 25 | 90 | 0.95 | 0.00398 | 19.7 | 450 | 6 |
| G6 | 80 | 20 | 40 | 0.74 | 0.00712 | 22.26 | 370 | 3 |
| G7 | 85 | 25 | 40 | 0.76 | 0.00079 | 27.74 | 480 | 3 |
| G8 | 55 | 10 | 40 | 0.65 | 0.00413 | 25.92 | 660 | 1 |
| G9 | 55 | 10 | 40 | 0.64 | 0.00222 | 27.27 | 665 | 1 |

### *4.2. Analysis of demand response results*

In this paper, a price-based demand response model is used to guide customers' electricity consumption behavior through a real-time tariff mechanism. The main diagonal element of the price-based elasticity matrix is -0.2 and the non-diagonal element is 0.033, and the electricity price before the response is a fixed tariff of 0.1 $/kWh. The electric load and real-time tariff after the response are shown in Figure 3 and Figure 4.

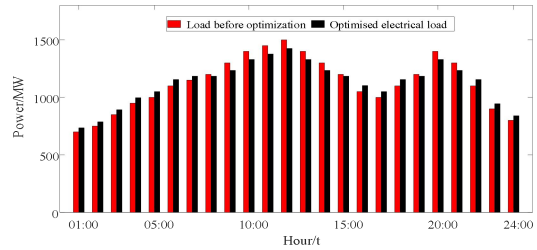


Fig.3 Load curve before and after response

As can be seen from Figure 3, the peak-to-valley difference of the load curve after demand response is reduced compared with the original load curve, and the load curve is optimized so that the peak loads in the 08:00-15:00 and 19:00-21:00 periods are shifted to the 22:00-07:00 and 16:00-18:00 periods, effectively reducing the peak-to-valley difference of the load.

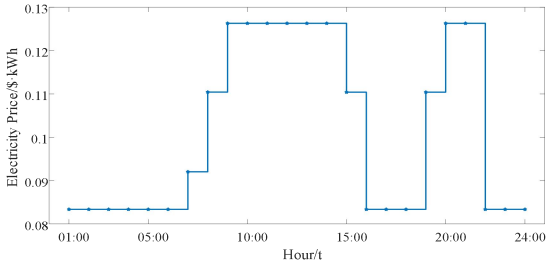


Fig.4 Real-time price after PDR

As can be seen from Figure 4, there is a negative correlation between users' electricity consumption behavior and tariff setting. The tariffs in the 22:00-07:00 and 16:00-18:00 periods are lower than the fixed tariffs, which guide users to increase their electricity consumption during the low tariff period; the tariffs in the 08:00-15:00 and 19:00-21:00 periods are higher than the fixed tariffs, which guide users to reduce their electricity consumption during this period and shift the transferable load in this period is transferred to the low tariff period.

### *4.3. Analysis of the results of different scenarios of operation*

In this paper, the linearized model is solved by invoking the CPLEX solver through the YALMIP toolbox, and the improved 10-unit transmission system is simulated with a 24h period and 1h step, and four scenarios are set up.

Scenario 1: Coordinated operation scenario of EV fixed charging and discharging price considering only demand response;

Scenario 2: Coordinated operation scenario considering demand response with EV charging and discharging peaking compensation mechanism;

Scenario 3: Considering coordinated operation scenarios of demand response with deep peaking mechanism considering clean emissions and EV fixed charging and discharging price;

Scenario 4: Consider the coordinated operation scheme of demand response and integrated operation mechanism.

Comparing the total cost under each scenario, the number of EV discharges, the wind power consumption rate, and the actual carbon

emissions, the results are shown in Table 3. The EV's orderly charging and discharging price are shown in Figure 5.

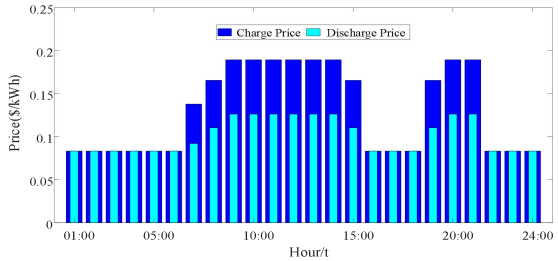


Fig.5 EV orderly charge and discharge price in Scenario 4

Tab.3 Optimized operating solutions results for different scenarios

| Scene classification | Total cost /$ | EV discharge quantity/vehicle | Wind power consumption rate/% | Actual carbon emissions/t |
|---|---|---|---|---|
| 1 | 1,031,054.41 | 12,770 | 80.45 | 26,559.36 |
| 2 | 835,149.46 | 45,000 | 75.54 | 26,193.01 |
| 3 | 1,024,845.37 | 23,473 | 100 | 22,515.56 |
| 4 | 801,907.16 | 45,000 | 100 | 22,134.03 |

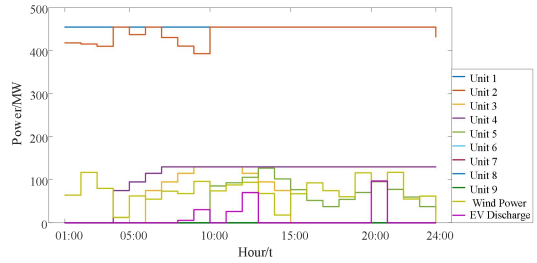


Fig.6 Optimized operating solutions results for scenario 1

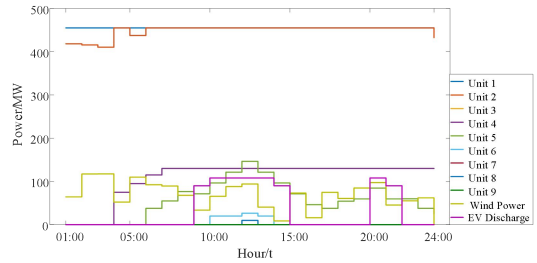


Fig.7 Optimized operating solutions results for scenario 2

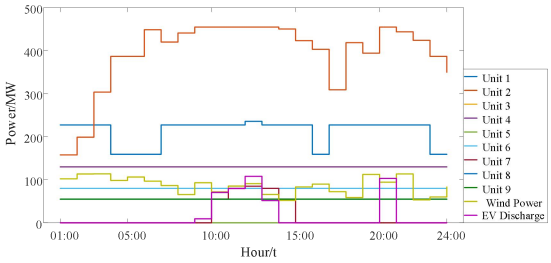


Fig.8 Optimized operating solutions results for scenario 3

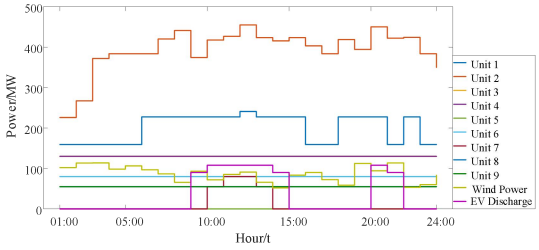


Fig.9 Optimized operating solutions results for scenario 4

From Figure 6, it can be found that in the fixed charge/discharge price unit combination model considering only demand response, units 1, 2, 3, 4, and 5 are on, with units 1 and 2 as base-load units and an entire generation, effectively improving the economics of the coordinated operation method; EV discharge is concentrated in peak load hours to obtain discharge revenue; as units 1 and 2 maintain base-load, they do not leave enough space for wind power feed-in, reducing the economics of the scheme. Due to the peak-shaving and valley-filling role of demand response, a particular space is left for wind power to go online, while EV charging and discharging behavior is equivalent to increasing the system's rotating standby, prompting wind power to be consumed, but the lack of peaking capacity of base-load units limits the system's use of wind power; as discharging causes battery losses, EV users discharge less and charging and discharging behavior is in line with residents' living habits.

From Figure 7, it can be found that the coordinated operation model considering only demand response and EV orderly charging and discharging peaking compensation mechanism, units 1, 2, 4, 5, 6 and 8 are on, and units 6 and 8 are used as flexible regulation units to meet load balancing. The charging time of electric vehicles is concentrated at 23:00-05:00 and 17:00, and

the discharging time is concentrated at 09:00-14:00 and 20:00-21:00, during which electric vehicles participate in auxiliary peaking to obtain maximum economic benefits. Too many vehicles are involved in the discharge, while Unit 1 is in full generation all day, and the peaking capacity is seriously insufficient, leaving not enough space for wind power to be connected to the grid, leading to a decrease in the wind power consumption rate compared to Scenario 1, and an increase in the cost of wind abandonment penalty, reducing the economics of the scheme.

From Figure 8, it can be found that the coordinated operation model considering only the deep peaking mechanism of demand response and clean emissions, units 1, 2, 3, 4, 6, 8 and 9 are on, and the output of unit 2 is flexibly adjusted under the influence of clean emissions, and low-carbon units 3, 4, 6, 8 and 9 are fully fired throughout the day, and the low-carbon nature of the system is greatly enhanced. EV charging time is mainly concentrated in 23:00-05:00, and discharging time is concentrated in 09:00-13:00 & 20:00. Considering the mobile energy storage characteristics of EV users, EV discharging is increased compared with Scenario 1 in order to meet the power balance. As Unit 1 is always in the deep peaking stage, it obtains deep peaking compensation, leaving enough space for wind power to be connected to the grid and increasing the system operation economy.

From Figure 9, it can be found that the optimized operation scheme of EV orderly charging and discharging price considering demand response and integrated operation mechanism needs to consider both the low carbon as well as economic aspects of the optimized operation scheme. Units 1, 2, 3, 4, 6, 8, and 9 are on power; under the influence of the deep peaking mechanism considering clean emissions, the power of high carbon emission units 1 and 2 is greatly reduced, low carbon units 3, 4, 6, 8, and 9 are in full power all day long to improve the low carbon and economic operation of the units, and units 5 and 7 have higher carbon emissions and their power cannot meet the load demand in the peak period, so units 5 and 7 are shut down. Unit 1 is always in the deep peaking stage to obtain peaking compensation and reduce carbon emission at the same time.With the reduction of total output of Units 1,2 base-load units, the flexibility of unit output is improved, leaving enough space for wind power to go online; at the same time, the system achieves total wind power consumption, gets more initial carbon emission allowances, reduces carbon penalty cost, and the orderly charging and discharging behavior of electric vehicle users gets tariff to guide auxiliary thermal units for deep peaking and obtains peaking compensation income.

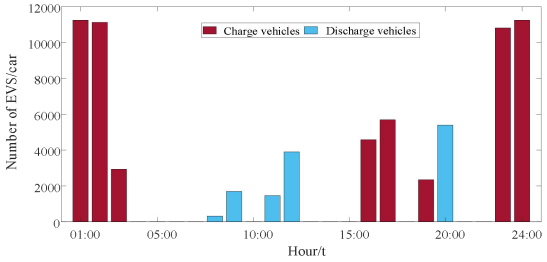


Fig.10 Distribution of EV charging and discharging quantity in Scenario 1

From Figure 10, it can be found that under a fixed charging and discharging price and no peaking compensation mechanism,charging vehicles are distributed at 23:00-03:00, 16:00-17:00 and 19:00; discharging vehicles are distributed at 08:00-09:00, 11:00-12:00 and 20:00. EV charging and discharging behavior is equivalent to acting as an energy storage unit, increasing system rotating backup, which can promote wind power consumption, but EV discharging will cause battery loss, user participation in discharging is low, the number of discharging users is low, and charging and discharging behavior is in line with residents' living habits.

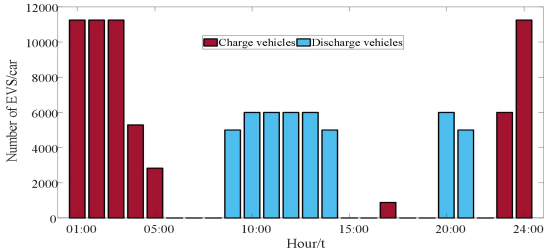


Fig.11 Distribution of EV charging and discharging quantity in Scenario 4

From Figure 11, Charging EVs are distributed in the low charging tariff 23:00-05:00 hours and 17:00 hours when EV charging costs are lowest; discharging EVs are

distributed in the high discharging tariff hours, i.e., 09:00-14:00 and 20:00-21:00 hours, when EV discharging revenues are highest; due to the discharging incentive compensation mechanism, EV users are attracted to At the same time, due to the discharge incentive compensation mechanism, EV users are attracted to discharge, which enhances their willingness to discharge and increases the number of EVs participating in the discharge behavior.

As can be seen from Table 3, scenario 4 compared to scenario 1, the total cost is reduced by 22.22%, the number of discharged EVs is increased by 32,230, the rate of wind power consumption is increased by 19.55%, and the actual carbon emission is reduced by 16.66%; compared to scenario 2, the total cost is reduced by 3.98%, the number of discharged EVs is the same, the rate of wind power consumption is increased by 24.46%, and the actual carbon emission is reduced by 15.49%; compared to scenario 3, the total operating cost is reduced by 21.75%, the number of discharged EVs is increased by 21,527, the wind power consumption rate is the same, and the actual carbon emissions are reduced by 1.69%; since Scenario 4 considers the orderly charging and discharging peaking compensation mechanism for electric vehicles, which enables the system to receive discharge compensation income from the electricity market, high-carbon units 1 and 2 significantly reduce their output, reducing carbon emissions and leaving enough space for wind power to connect to the grid. Due to the comprehensive consideration of the deep peaking mechanism for clean emissions and the orderly charging and discharging peaking compensation mechanism, Scenario 4 has the lowest cost and carbon emissions and the highest wind power consumption rate.

### *4.4. Analysis of EV charging and discharging behavior on distribution network loss results*

In this paper, we use the IEEE 33-node distribution network to simulate the calculation of EV charging and discharging behavior on the network loss of the distribution network, assuming that 5% of EVs in the transmission system are distributed in this distribution network, and the distribution network is shown in Figure 12, and 2 scenarios are set.

Scenario 5: the distribution network does not contain EVs.

Scenario 6: The distribution network contains EVs, and the EV charging and discharging time follows the EV charging and discharging time of scenario 4.

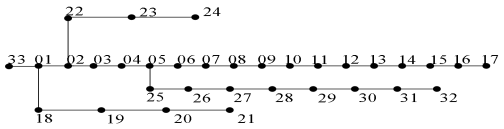


Fig.12 IEEE33-node distribution network topology

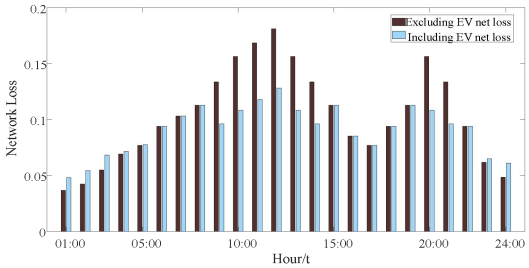


Fig.13 Influence curve of EV on distribution network loss

The impact of EV on the distribution network loss is shown in Figure 13, in which the network loss of the distribution network without EV is 2.4964MW and the network loss of the distribution network with EV is 2.1915MW, and the network loss of the distribution network is reduced by 13.91%, indicating that adding EV to the distribution network and doing proper planning for the charging and discharging behavior of EV can effectively reduce the network loss of the distribution network and optimize the distribution network tide distribution.

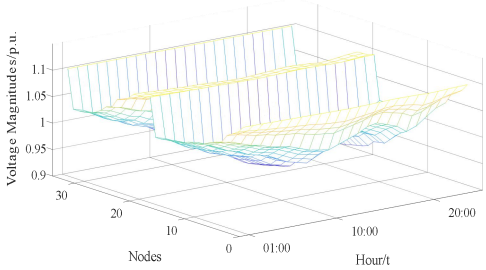


Fig.14 Voltage level for scenario 5

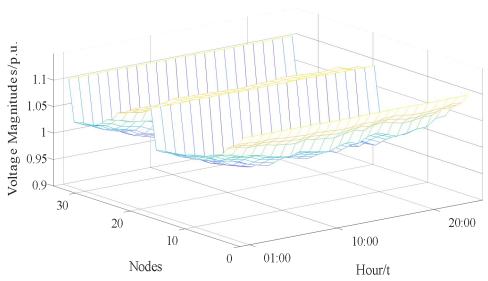


Fig.15 Voltage level for scenario 6

Comparing Fig. 14 and 15, it can be found that in the distribution network without EVs, the voltage at the nodes closer to the busbar is higher than the voltage at the end nodes; the distribution network with EVs can make use of the mobile energy storage characteristics of EVs to arrange EVs with the willingness to discharge to the end nodes for discharging, to support the voltage at the end nodes and avoid voltage collapse. In contrast, EVs desiring to charge are dispatched to the first node for charging to avoid the impact of disorderly charging and discharging of EVs on the voltage level of the distribution network.

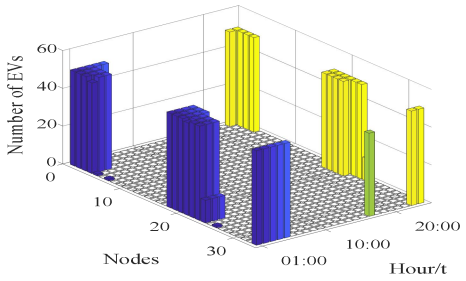


Fig.16 Temporal and spatial distribution of charge vehicles in distribution network

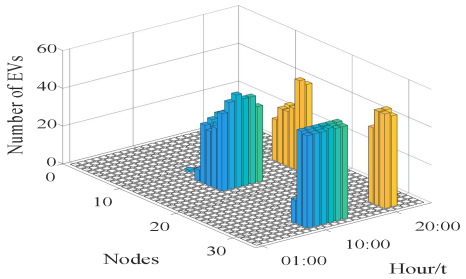


Fig.17 Temporal and spatial distribution of discharge vehicles in distribution network

From Figures 16 and 17, it can be seen that charging vehicles are distributed between 17:00 and 23:00-05:00 in time and spatially distributed in the nodes at the head end of the distribution network; discharging vehicles are distributed between 09:00-14:00 in time And 20:00-21:00, spatially distributed at the end nodes of the distribution network, which can effectively reduce the net loss of the distribution network and improve the operation economy of the distribution network.

To sum up the above analysis, it can be seen that the model established in this paper combines price-based demand response, deep peaking mechanism considering clean emissions, and orderly charging and discharging peaking compensation mechanism to make the coordinated operation method play a role in promoting low-carbon emission reduction, improving the utilization rate of new energy, and improving the system economy. At the same time reduce the network loss of the distribution network.

## 5. Conclusion

Under the background of "double carbon," in order to improve the utilization rate of new energy, reduce carbon emissions and rationalize the use of low-carbon resources such as EVs, this paper proposes a three-stage coordinated operation model considering demand response, deep peaking mechanism considering clean emissions and orderly charging and discharging peaking compensation mechanism from the source network, load and storage aspects, and obtains the following conclusions:

(1) To build a model of coordinated operation of source, network, load, and storage resources that considers the characteristics of electric vehicle mobile energy storage, which can effectively improve the economy and low carbon of system operation and reduce the network loss of distribution network operation.

(2) Considering the cost of EV discharging losses, EV users are not willing to participate in discharging behaviors. By deriving orderly charging and discharging prices through price-based demand response, the economy of the coordinated operation method is effectively enhanced through a combination of peak compensation compensation mechanisms and mechanisms that consider clean emissions, while increasing users' willingness to discharge and reducing carbon emissions.

(3) Compared with the demand response and fixed charging and discharging mechanism models, the three-stage coordinated operation method model proposed in this paper, which

takes into account the low-carbon characteristics of EVs, reduces the total cost by 22.22%%, increases the number of EVs involved in discharging by 32,230, improves the wind power consumption rate by 19.55% and reduces carbon emissions by 16.66%, effectively improving the economy of system operation and low-carbon performance.

(4) Through rational planning of EV charging and discharging behavior, the tidal distribution of the distribution network can be optimized, and the network loss of the distribution network containing EVs is reduced by 13.91%.

This paper proposes a three-stage coordinated operation method that considers the source-grid load and storage resources, which can significantly improve the wind power consumption rate, effectively enhance the economics and low carbon of the coordinated operation method, and reduce the network loss of the distribution network.

**Acknowledgments**

This work was financially supported by the Shaanxi Provincial Education Department Scientific Research Program Project (21JK0843) and National Natural Science Foundation of China (52174005).

**References**

[1] R. Wang, X. Wen, X. Wang, Y. Fu, and Y. Zhang, "Low carbon optimal operation of integrated energy system based on carbon capture technology, LCA carbon emissions and ladder-type carbon trading," *Applied Energy,* vol. 311, p. 118664, 2022/04/01/ 2022, doi: https://doi.org/10.1016/j.apenergy.2022.118664.

[2] X. Liu, X. Li, J. Tian, and H. Cao, "Low-carbon economic dispatch of integrated electricity and natural gas energy system considering carbon capture device," *Transactions of the Institute of Measurement and Control,* p. 01423312211060572, 2021, doi: 10.1177/01423312211060572.

[3] J. Qiu, Z. Xu, Y. Zheng, D. Wang, and Z. Y. Dong, "Distributed generation and energy storage system planning for a distribution system operator," *IET Renewable Power Generation,* https://doi.org/10.1049/iet-rpg.2018.5115 vol. 12, no. 12, pp. 1345-1353, 2018/09/01 2018, doi: https://doi.org/10.1049/iet-rpg.2018.5115.

[4] N. Pathak and Z. C. Hu, "Optimal power flow of MT-HVDC system connected large offshore wind farms using mixed-integer semi-definite programming approach," *Iet Generation Transmission & Distribution,* vol. 15, no. 3, pp. 456-467, Feb 2021, doi: 10.1049/gtd2.12033.

[5] M. Chen, H. Lu, X. Chang, and H. Liao, "An optimization on an integrated energy system of combined heat and power, carbon capture system and power to gas by considering flexible load," *Energy,* vol. 273, p. 127203, 2023/06/15/ 2023, doi: https://doi.org/10.1016/j.energy.2023.127203.

[6] M. R. Kikhavani, A. Hajizadeh, and A. Shahirinia, "Charging coordination and load balancing of plug-in electric vehicles in unbalanced low-voltage distribution systems," *Iet Generation Transmission & Distribution,* vol. 14, no. 3, pp. 389-399, Feb 2020, doi: 10.1049/iet-gtd.2019.0397.

[7] M. Du, Y. G. Niu, B. Hu, G. P. Zhou, H. H. Luo, and X. Qi, "Frequency regulation analysis of modern power systems using start-stop peak shaving and deep peak shaving under different wind power penetrations," *International Journal of Electrical Power & Energy Systems,* vol. 125, Feb

2021, Art no. 106501, doi: 10.1016/j.ijepes.2020.106501.

[8] Z. P. Hong, Z. X. Wei, J. L. Li, and X. J. Han, "A novel capacity demand analysis method of energy storage system for peak shaving based on data-driven," *Journal of Energy Storage,* vol. 39, Jul 2021, Art no. 102617, doi: 10.1016/j.est.2021.102617.

[9] S. Wang, F. T. Li, G. H. Zhang, and C. Y. Yin, "Analysis of energy storage demand for peak shaving and frequency regulation of power systems with high penetration of renewable energy," *Energy,* vol. 267, Mar 2023, Art no. 126586, doi: 10.1016/j.energy.2022.126586.

[10] Z. Wu, J. Li, and M. Li, "Multi-Alliance Market Subject Auxiliary Peak Shaving Strategy for New Energy Consumption," in *2023 8th Asia Conference on Power and Electrical Engineering (ACPEE)*, 14-16 April 2023 2023, pp. 892-898, doi: 10.1109/ACPEE56931.2023.10135915.

[11] X. Y. Wang, Y. T. Wu, and L. Fu, "Configuration method for combined heat and power plants with flexible electricity regulation," *Energy and Buildings,* vol. 287, May 2023, Art no. 112966, doi: 10.1016/j.enbuild.2023.112966.

[12] Q. Tang, M. Xie, K. Yang, Y. Luo, D. Zhou, and Y. Song, "A Decision Function Based Smart Charging and Discharging Strategy for Electric Vehicle in Smart Grid," *Mobile Networks and Applications,* vol. 24, no. 5, pp. 1722-1731, 2019/10/01 2019, doi: 10.1007/s11036-018-1049-4.

[13] Y. He, B. Venkatesh, and L. Guan, "Optimal Scheduling for Charging and Discharging of Electric Vehicles," *IEEE Transactions on Smart Grid,* vol. 3, no. 3, pp. 1095-1105, 2012, doi: 10.1109/TSG.2011.2173507.

[14] E. Apostolaki-Iosifidou, P. Codani, and W. Kempton, "Measurement of power loss during electric vehicle charging and discharging," *Energy,* vol. 127, pp. 730-742, 2017/05/15/ 2017, doi: https://doi.org/10.1016/j.energy.2017.03.015.

[15] W. Yin and X. Qin, "Cooperative optimization strategy for large-scale electric vehicle charging and discharging," *Energy,* vol. 258, p. 124969, 2022/11/01/ 2022, doi: https://doi.org/10.1016/j.energy.2022.124969.

[16] G. Merhy, A. Nait-Sidi-Moh, and N. Moubayed, "Control, regulation and optimization of bidirectional energy flows for electric vehicles' charging and discharging," *Sustainable Cities and Society,* vol. 57, p. 102129, 2020/06/01/ 2020, doi: https://doi.org/10.1016/j.scs.2020.102129.

[17] R. Tang, S. Wang, and H. Li, "Game theory based interactive demand side management responding to dynamic pricing in price-based demand response of smart grids," *Applied Energy,* vol. 250, pp. 118-130, 2019/09/15/ 2019, doi: https://doi.org/10.1016/j.apenergy.2019.04.177.

[18] R. Lu, S. H. Hong, and M. Yu, "Demand Response for Home Energy Management Using Reinforcement Learning and Artificial Neural Network," *IEEE Transactions on Smart Grid,* vol. 10, no. 6, pp. 6629-6639, 2019, doi: 10.1109/TSG.2019.2909266.

[19] M. A. S. Hassan *et al.*, "Dynamic Price-Based Demand Response through Linear Regression for Microgrids with Renewable Energy

Resources," *Energies,* vol. 15, no. 4, p. 1385, 2022. [Online]. Available: https://www.mdpi.com/1996-1073/15/4/1385.

[20] M. A. Mirzaei, A. Sadeghi Yazdankhah, and B. Mohammadi-Ivatloo, "Stochastic security-constrained operation of wind and hydrogen energy storage systems integrated with price-based demand response," *International Journal of Hydrogen Energy,* vol. 44, no. 27, pp. 14217-14227, 2019/05/24/ 2019, doi: https://doi.org/10.1016/j.ijhydene.2018.12.054.

[21] Y. Li, M. Han, Z. Yang, and G. Li, "Coordinating Flexible Demand Response and Renewable Uncertainties for Scheduling of Community Integrated Energy Systems With an Electric Vehicle Charging Station: A Bi-Level Approach," *IEEE Transactions on Sustainable Energy,* vol. 12, no. 4, pp. 2321-2331, 2021, doi: 10.1109/TSTE.2021.3090463.

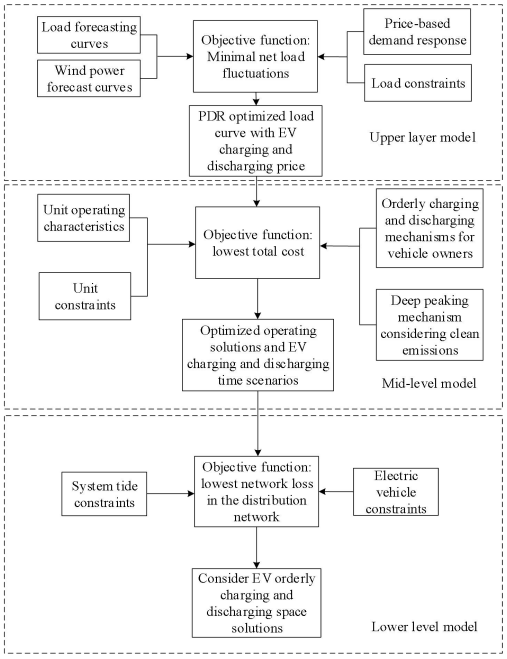


Fig.1 A three-stage optimal operation model of source-grid-load-storage considering the mobile energy storage characteristics of electric vehicles

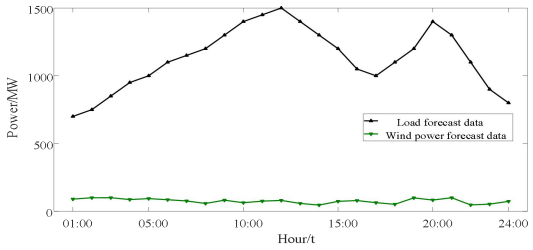


Fig.2 Load and wind power forecasting

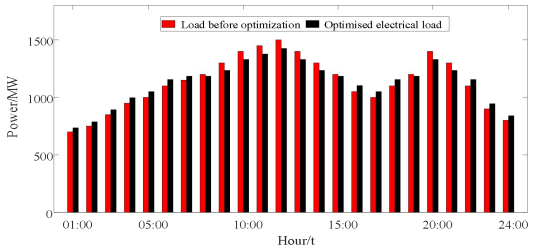


Fig.3 Load curve before and after response

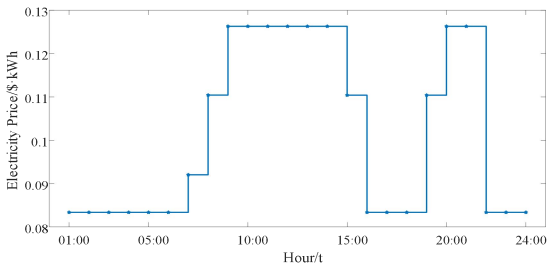


Fig.4 Real-time price after PDR

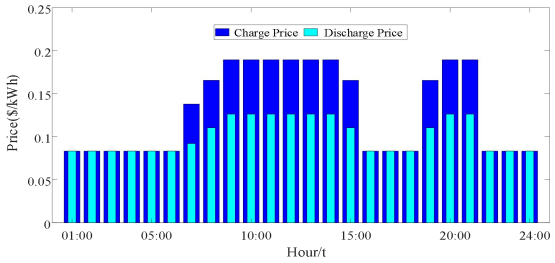


Fig.5 EV orderly charge and discharge price in Scenario 4

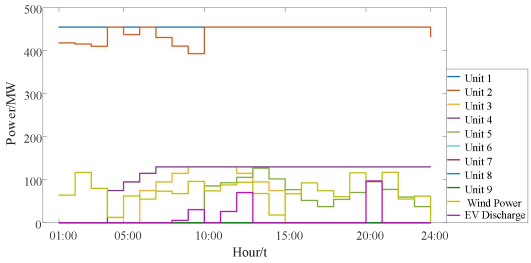


Fig.6 Optimized operating solutions results for scenario 1

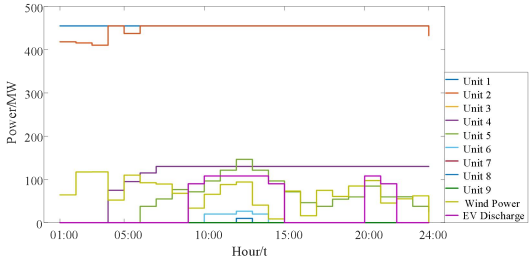


Fig.7 Optimized operating solutions results for scenario 2

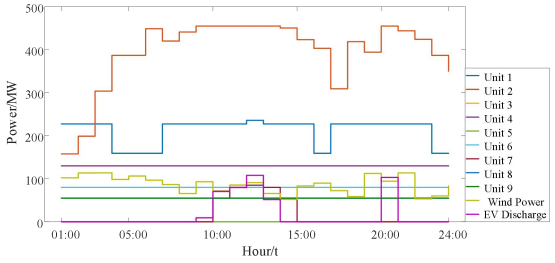


Fig.8 Optimized operating solutions results for scenario 3

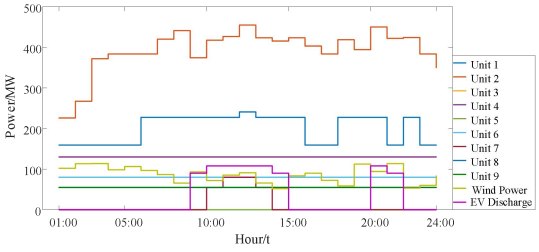


Fig.9 Optimized operating solutions results for scenario 4

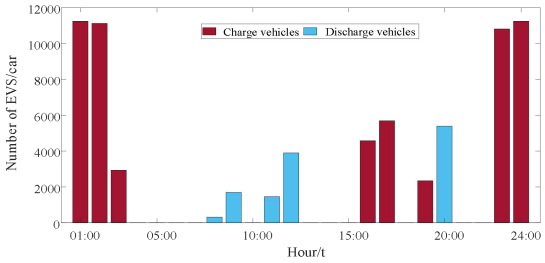


Fig.10 Distribution of EV charging and discharging quantity in Scenario 1

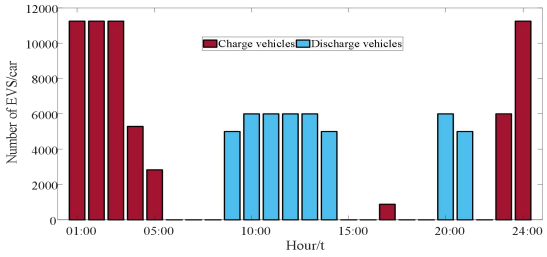


Fig.11 Distribution of EV charging and discharging quantity in Scenario 4

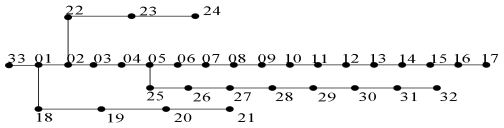


Fig.12 IEEE33-node distribution network topology

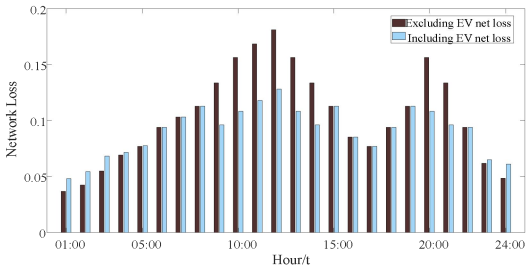


Fig.13 Influence curve of EV on distribution network loss

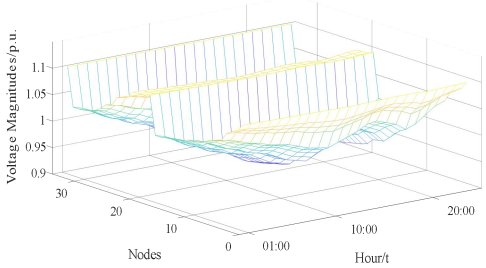


Fig.14 Voltage level for scenario 5

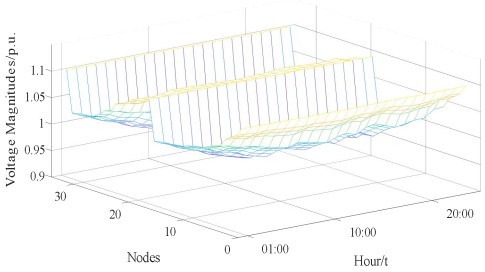


Fig.15 Voltage level for scenario 6

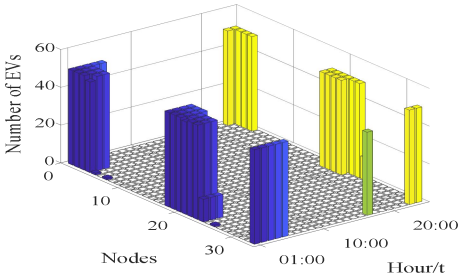


Fig.16 Temporal and spatial distribution of charge vehicles in distribution network

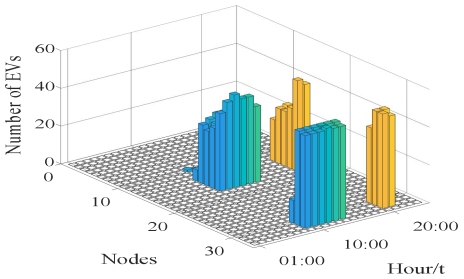


Fig.17 Temporal and spatial distribution of discharge vehicles in distribution network